# Comb-Generator Characterization

Howard Charles Reader, Dylan F. Williams, *Fellow, IEEE*,
Paul D. Hale, *Senior Member, IEEE*, and Tracy S. Clement, *Senior Member, IEEE*

*Abstract*—We characterize a 50-GHz comb generator with a sampling oscilloscope. With careful control of the input power, input harmonics, and comb generator temperature, we measure the output spectrum with a standard uncertainty of 0.1 dB and 0.5°. We correct the measurements for time-base distortion, impedance mismatch, an inline attenuator, and the complex frequency response of the oscilloscope's sampler. We also report on the stability of the comb-generator spectrum and the effects of the recorded time windows, drive levels, and temperature. These results provide general guidelines for practioners of high-speed measurements and a benchmark for future inter-laboratory comparisons of harmonic phase-reference calibrations.

*Index Terms*—Comb-generator stability, mismatch correction, sampling-oscilloscope calibration.
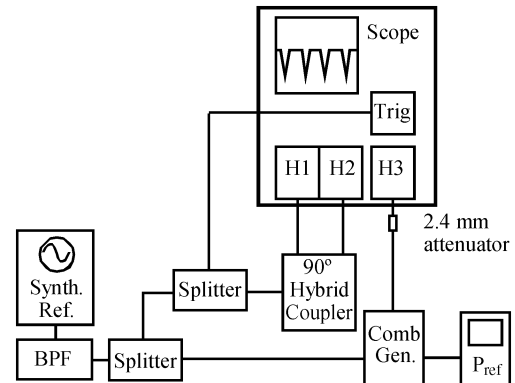
Fig. 1. Sampling oscilloscope with a 20-GHz two-channel plug-in (H1 and H2) to record the reference quadrature sinusoids and a 50-GHz plug-in (H3) to record the comb-generator signal. The input power is monitored on the meter $P_{\text{ref}}$. The attenuator is chosen to optimize signal levels to the 50-GHz plug-in.

## I. INTRODUCTION

**W**E USED a calibrated sampling oscilloscope to characterize both the magnitude and phase response of a comb generator whose spectral amplitude components at 50 GHz are 10 dB below their low-frequency levels. We corrected the measurements for impedance mismatch and distortion in the oscilloscope time base, achieving exceptionally high accuracy.

As the name implies, a comb generator produces a set (or "comb") of discrete harmonically related tones in the frequency domain, corresponding to a periodic waveform in the time domain. The generator consists of one or more nonlinear elements, such as a step recovery diode and a nonlinear transmission line, and a passive pulse-forming network that transforms a sinusoidal input into a periodic signal rich in harmonics.

Historically, comb generators were used as harmonic signal sources in phase-locked loops or in electromagnetic interference (EMI) testing and spectrum analyzer calibration. For these applications, only the comb generator's magnitude was characterized [1], [2]. Recently, comb generators have found wide use as a transfer standard for calibrating the phase response of signal measurement instrumentation, such as oscilloscopes, vector signal analyzers, and large signal network analyzers

[3]–[5]. These new applications require a transfer standard in which the relative phase of each harmonic component has been calibrated.

We measured a comb generator's response on a sampling oscilloscope mainframe with two separate 50-GHz plug-ins at the National Institute of Standards and Technology (NIST), Boulder, CO. We first compensated for the random and systematic errors in the oscilloscope's time base using the algorithm [6] implemented in the NIST time-base correction software [7]. We then removed the effects of impedance mismatches between the comb generator and oscilloscope plug-ins, and also corrected for an inline attenuator and the complex frequency response of the oscilloscope's sampler. The latter was determined through a combination of a swept-sine calibration [8] at low frequencies, merged with a traceable electrooptic-sampling-system phase calibration [9], [10].

We examined the magnitude and phase of the voltage that the comb generator delivers to an ideal 50-$\Omega$ load at its coaxial output under different operating conditions. The variations include experimental reproducibility, differences between oscilloscope plug-ins (samplers), choice of time window, drive-power levels, and ambient temperature.

## II. MEASUREMENT CONFIGURATION AND DATA PROCESSING

Fig. 1 shows our measurement configuration. A sinusoidal source is required to drive the comb generator. We used a synthesized reference generator to provide the 800-MHz drive for the comb generator. A bandpass filter was included to keep all higher order input harmonic levels 60 dB below the fundamental.

We used two splitters to derive the oscilloscope trigger and the two quadrature timing signals from a 90° hybrid coupler from the comb generator's drive signal. The two quadrature

timing signals are used to correct the oscilloscope's time base with the approach of [7].

We also set the power of the reference signal and calibrated attenuator to maintain the peak amplitude of the comb generator close to 150 mV. This minimizes small nonlinearities in the oscilloscope associated with the operating point of the sampling diodes [9]. An extensive reference on oscilloscope nonlinearities can be found in [11].

### A. Time-Base Correction Algorithm

We apply the two quadrature signals so that the NIST time-base correction algorithm can be used. That algorithm requires that we record these sinusoids and the comb generator pulse simultaneously [6]. With the scheme shown in Fig. 1, all the waveforms are synchronized to the reference source. A two-channel 20-GHz plug-in (indicated as H1 and H2 in Fig. 1) captures the quadrature signals.

The time-base correction algorithm uses an orthogonal-distance-regression method (also called an "error-in-variables method") to fit the sinusoids. The fit also allows for harmonic distortion in the quadrature signals to an arbitrary harmonic. In this study, we assume that three harmonics are adequate [12] to capture distortion due to the oscilloscope. The algorithm estimates random timing errors (jitter) by exploiting the fact that all the samplers in the oscilloscope are activated simultaneously by a strobe pulse from the oscilloscope's time base and that the sampling jitter is dominated by errors in the strobe pulse timing. The actual sampling time is estimated from the residuals of the fit and is used to correct timing errors in the recorded pulse. The corrected data is then linearly interpolated onto a regular time grid before transforming to the frequency domain by applying a fast Fourier transform algorithm.

A second form of the algorithm, which we refer to here as the "robust form," first estimates the deterministic error from time-base distortion and then uses that error as an initial guess for the total timing error. Estimating the time-base distortion requires that two additional quadrature-waveform sets, which are not harmonically related to the 800 MHz of the fundamental signal, also be acquired. These sinusoids are not recorded at the same time as the signal of interest.

Section III-A discusses why it is important to use the robust method. More details on the robust method and on the time-base correction algorithm are given in [6].

### B. Comb-Generator Recording and Initial Processing

Before recording the comb generator's temporal output signal for further processing, we ran the internal oscilloscope calibration routine on the 50-GHz plug-in (H3) with nothing connected to its input. This sets dc voltage levels and corrects for gain errors, offset errors, and some amplitude nonlinear distortion [9]. We also measured the remaining additive noise level and found that it was of the order of 500 $\mu$V rms. The quantization noise is substantially lower than this value and can be ignored.

In the measurements, we recorded four complete comb generator pulses, each having a period of 1.25 ns. We ensured that voltages were flat at the beginning and end of the full measurement period, which facilitates interpolation and reduces error in the discrete Fourier transform.
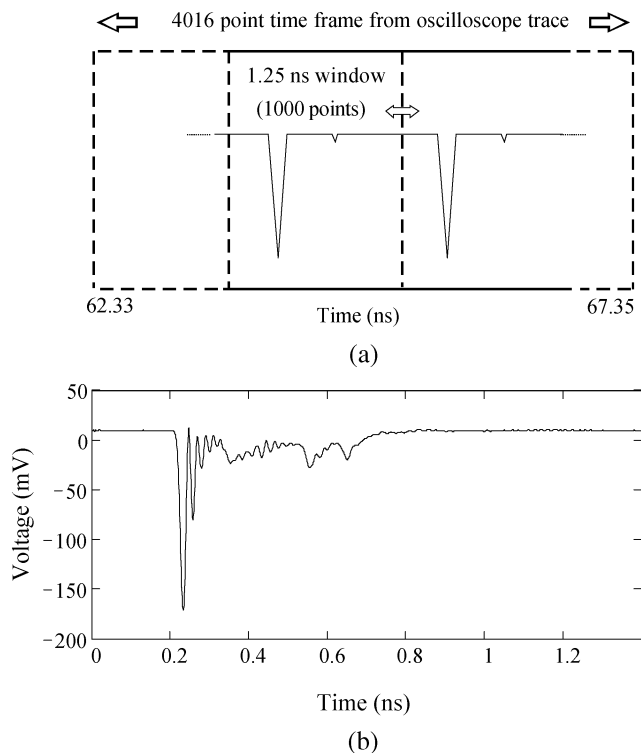


Fig. 2  (a) Oscilloscope 62.33–67.35-ns time frame recorded (schematic). The 1.25-ns window can be shifted within the time frame as desired. (b) Isolated single raw pulse as recorded on the oscilloscope.

Fig. 2 illustrates the measurement time frame, an individual window and our comb generator pulse. We selected the starting point of the time frame to be in a known region of time-base stability in order to simplify the estimation of the oscilloscope's time-base distortion. With 4016 samples, which are more samples than needed, two points are separated by 1.25 ps. The 800-MHz quadrature sinusoids were stored under exactly the same time conditions. We did not plot these quadrature signals in Fig. 2(b) to simplify the graph.

We acquired 100 repeated time frames in a short period and corrected each data file offline for time-base jitter, drift, and distortion using the NIST time-base correction algorithm [7]. We then interpolated the data to a regular grid and averaged the 100 waveforms, giving a 20-dB signal-to-noise ratio improvement. We chose the 1000-point window, seen in Fig. 2(a), to include or avoid the time-base reset that appears every 4 ns after the time reference of 22 ns on this oscilloscope. The window we selected also does not incorporate the first and last few points of the stored time frame, as these can be distorted by the interpolation procedure. This choice of window results in a frequency of 800 MHz.

Drift (time shift) can occur between different experiments recorded hours or days apart. We removed the drift by detrending the phase in the frequency domain. We did this by subtracting a linearly increasing phase from the phase data that minimized the phase differences over the entire range of frequencies. This is equivalent to a shift in the time domain and amounts to a realignment of the pulses so that they all peak at the same relative time.
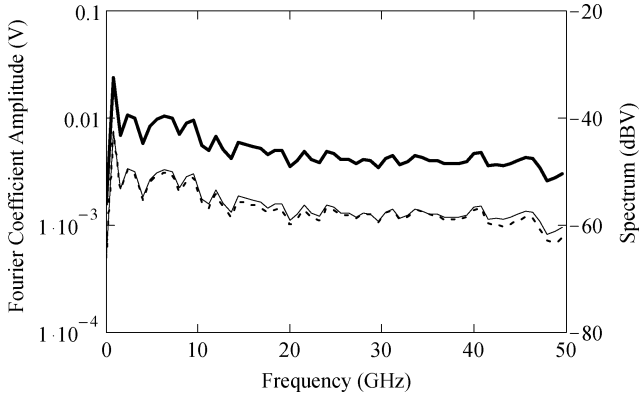
Fig. 3. Corrected comb generator spectrum $v_g$ magnitude in the bold trace. The thinner solid trace is $v_g$ shifted down by 10 dB and can be compared to the uncorrected impedance-mismatch spectrum of the dotted–dashed trace.



Fig. 4. Comb generator spectrum $v_g$ phase. The result has been detrended to give an approximately flat phase response from low to midfrequency.

## C. Data Correction

We applied frequency-domain impedance mismatch corrections to accommodate the small impedance differences between the oscilloscope plug-in and comb generator. We removed the effect of the 2.4-mm 10-dB attenuator at the comb generator output so that the voltage could be referred to the generator's coaxial connector plane. We also accounted for the complex frequency response of the plug-in.

By use of a standard flow diagram analysis, the voltage $v_g$ delivered to a perfect 50-$\Omega$ load by the generator can be determined from [13]

$$v_g = v_s \left( \frac{1 - \Gamma_g S_{11} - \Gamma_s S_{22} - \Gamma_g \Gamma_s (S_{21} S_{12} - S_{11} S_{22})}{S_{21} h} \right) \tag{1}$$

where $v_s$ is the voltage measured on the oscilloscope (time-base corrected and transformed to frequency domain), $\Gamma_g$ is the output reflection coefficient of comb generator, $\Gamma_s$ is the input reflection coefficient of oscilloscope plug-in, $S_{nn}$ are the $S$-parameters of the 2.4-mm 10-dB attenuator, and $h$ is the complex frequency response of the oscilloscope plug-in, as determined by the techniques of [9] and [13].

We measured the reflection coefficients of the comb generator and plug-ins, and the $S$-parameters of the 2.4-mm attenuator on a calibrated vector network analyzer using an 800-MHz grid up to 50 GHz. We obtained the dc points separately with a calibrated ohmmeter and transformed into $S$-parameters.

## III. COMB GENERATOR SPECTRAL CHARACTERISTICS UNDER DIFFERENT CONDITIONS

In this discussion, we present the dc point and positive Fourier coefficients. This avoids any ambiguity involved in presenting a combination of positive and negative Fourier coefficients. The sampled comb generator pulse is real and periodic with finite power so the time waveform and Fourier amplitude coefficients have the same units of volts [13]. When these coefficients are plotted, we show the linear amplitude on the left-hand vertical axis and the decibel value on the right-hand axis.

The bold upper trace in Fig. 3 shows the comb generator spectrum magnitude after having applied all the corrections of (1). This is effectively the voltage delivered to an ideal 50-$\Omega$ load
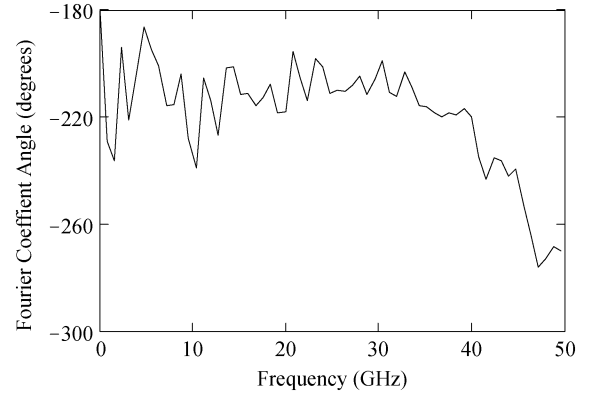
at the coaxial connector plane. For comparison, we depict the uncompensated frequency domain data (dotted–dashed trace) against the corrected data as though the 10-dB 2.4-mm attenuator were perfect (thin solid trace). The latter traces give a good indication of the level of amplitude correction introduced by the impedance mismatch removal process.

We show the phase of the corrected spectrum in Fig. 4. The value at dc is retained in the correction process since the $S$-parameters of all the devices have been explicitly measured there. The negative-going pulse of Fig. 2 gives rise to the $-180°$ phase at the dc point. In presenting the result, we unwrap the Fourier coefficient angles and detrend the phase with a constant-slope line, as in Section II-B.

We now examine the effects of different data-processing and operating conditions on the comb generator. We use the magnitude and phase plots of Figs. 3 and 4 as our reference.

## A. Data Processing and Repeatability

We explored the parameters of the time-base correction algorithm and repeatability. In our principal test, we studied the generator under identical experimental conditions, utilizing the two 50-GHz plug-ins, on separate occasions, over a period of two weeks. Fig. 5 shows data from six reconnected measurements that we processed using the simple form of the algorithm, followed by mismatch correction. The largest changes are between the two plug-ins from different days.

Although the difference at dc is 4 dB, it is due only to a small overall drift in the oscilloscope voltage levels. These oscilloscope levels are sensitive to the internal oscilloscope level calibration, which can be repeated several times to eliminate the observed difference.

When using the time-base correction algorithm, we must choose a weighting between our confidence in the time base of the oscilloscope and the recorded voltage amplitudes. We optimized this weighting choice following the recommendations provided in [6]. We found that a nonoptimal choice of this weighting factor can affect the phase results by up to 3° in the basic form of the algorithm.

The worst case results in Fig. 5 appear to be large, up to 2 dB and 10° across the 50-GHz band. It should be noted that these first results are not solely a function of the comb generator stability. The simple form of the time-base correction algorithm
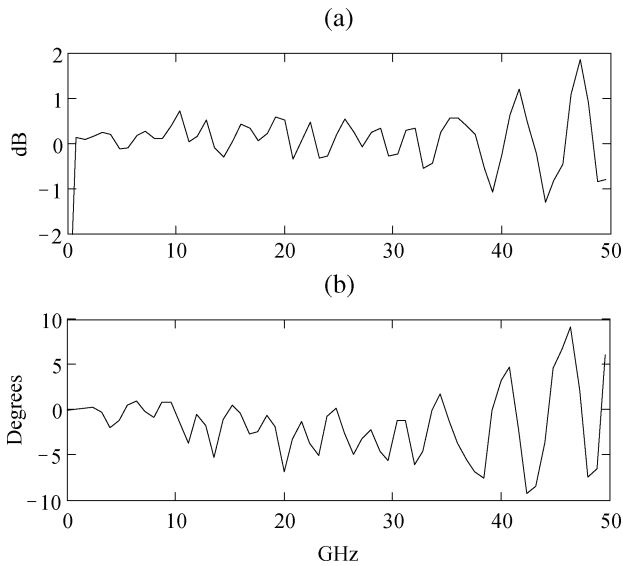
Fig. 5. Largest difference between six identical measurements of the comb generator taken on the two plug-ins days apart when the simple form of the algorithm is used. (a) Difference in decibel magnitude and (b) phase difference. Significantly improved results due to the robust algorithm are shown in Fig. 6.

TABLE I
STANDARD UNCERTAINTY ($1\sigma$) OF THE FREQUENCY RESPONSE MAGNITUDE
AND PHASE FOR THE TWO PLUG-INS IN FREQUENCY BANDS USED [9]

|                     | 0 – 32 GHz | 32 – 40 GHz | 40 – 50 GHz |
|---------------------|-----------|-------------|-------------|
| Magnitude std. unc. | 0.17      | 0.28        | 0.34        |
| Phase std. unc.     | 1°        | 1.7°        | 2.3°        |

also affects the findings. We determined the standard deviation of the mean, or type A standard uncertainty [14], for the six measurements to be 0.33 dB in magnitude and 2° in phase across the band. The values just fall within the quoted standard uncertainty data for the two plug-ins used [9], which are summarized in Table I.

Thus far, we have used the simple form of the time-base correction algorithm, which assumes Gaussian noise for the time-base distortion. This is not true for the mainframe used. The time reset every 4 ns is significantly nonlinear.

The robust algorithm uses two other nonharmonically driven waveforms to estimate the time-base distortion. To test and demonstrate the importance of using the robust method, we performed five new experiments with the two 50-GHz plug-ins on different days and also recorded the extra nonharmonically related waveforms at 847 and 907 MHz.

With the additional robust information, the standard deviations are far improved to 0.08 dB in magnitude and 0.4° in phase at 50 GHz. In Fig. 6, we show the *largest* difference between the comb generator results taken on the same mainframe between the two plug-ins on different days.

The maximum variations in Fig. 6, ignoring the dc point, are 0.3 dB and 1.5°. These are comparatively small. The result gives a good indication of how well the plug-ins' complex frequency responses have been determined and what levels of repeatability can be achieved between reconnected experiments.
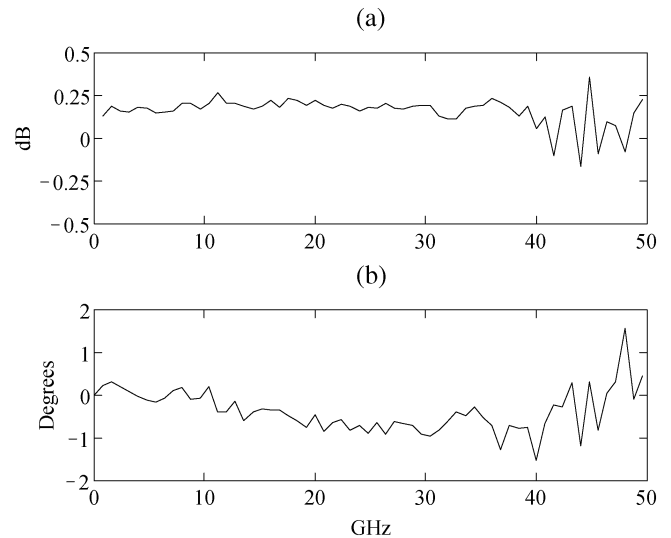


Fig. 6. Largest difference between five identical measurements of the comb generator taken on the two plug-ins days apart. The robust algorithm is used. Difference in: (a) decibel magnitude and (b) phase.

We thus adopted the robust form of the algorithm, which requires that the nonharmonic waveforms be recorded during the measurement sequence as our standard algorithm.

### B. Time-Window Choice

One of the four recorded time frames in Fig. 2 contains a time-base reset. We have measured sampling-time jumps of approximately 40 ps due to these time-base resets. The time-base algorithm [6] corrects for this, as well as random and systematic timing errors. We should then be able to use any one of the four recorded pulses to test the stability of our comb generator.

To verify this, we took a single data file and processed the data as described in Section II. Each of the four possible time windows was selected in turn, avoiding the first and last 50 data points of each time frame to minimize interpolation errors. We then compared each of the four possibilities and found that the standard deviations in magnitude and phase are 0.015 dB and 0.09° over the band. This indicates that the robust algorithm performs well across the entire time frame and corrects for time-base resets.

### C. Drive-Power Stability

The comb generator has a first stage amplifier that operates in extreme saturation so as to reduce the influence of its drive levels. To test the stability and effectiveness of this circuit, we performed a series of measurements in which we varied only the drive power. We controlled the synthesized generator, seen in Fig. 1, to an accuracy of 0.1 dB using a power meter. Fig. 7 shows the results when the power was decreased by 0.1 dB from its nominal value of −0.8 dBm.

We see that the measured differences are as large as 0.6 dB and 1.9°, exceeding those due to plug-in and re-connection changes (0.3 dB and 1.5°). Changes of drive power of 0.2 dB increase these differences to 1 dB and 2.5°. These experiments indicate that drive levels need to be controlled to better than 0.1 dB to obtain even modest accuracy in the results.
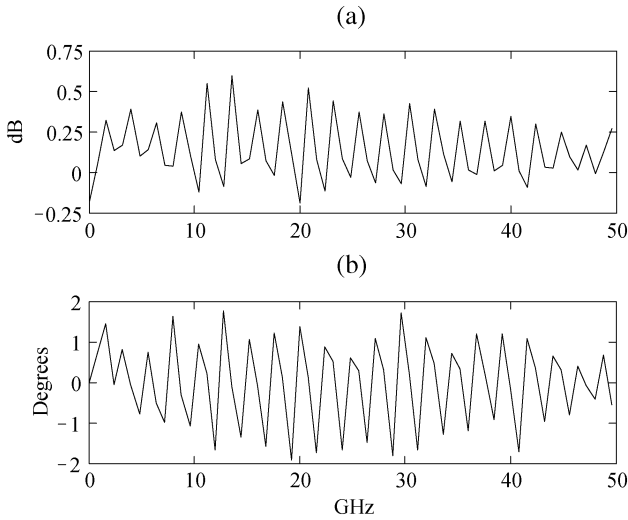
Fig. 7. Difference in comb-generator results from the same experiment with the driving power decreased by 0.1 dB. The robust time-base correction algorithm was used. (a) Magnitude (decibel) difference. (b) Phase difference.
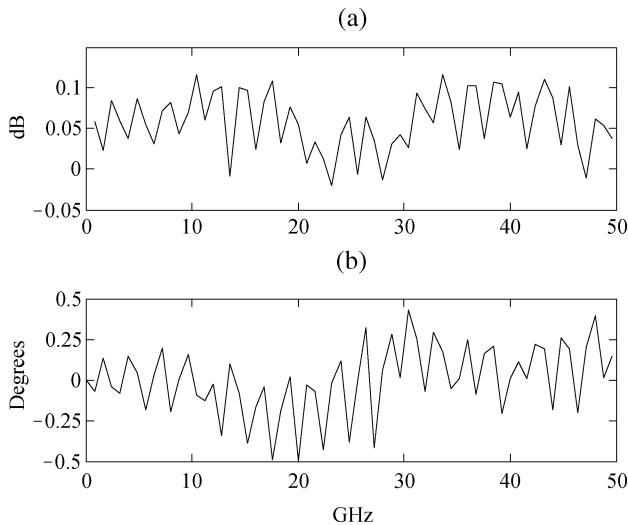


Fig. 8. Difference in comb generator results from the same experiment with the temperature changed by 2.5 K. The robust algorithm was used. (a) Magnitude (decibel) difference. (b) Phase difference.

## D. Temperature Stability

We examined the temperature stability of the comb generator by wrapping the generator in a thermal blanket. This raised its temperature by 2.5 K as measured by a calibrated thermocouple taped firmly to the generator's metallic chassis. The temperature was left to equilibrate for several hours before any results were recorded.

Fig. 8 shows the change due to the temperature increase. Apart from the dc point, the differences with the 2.5 K increase are seen to be less than 0.15 dB and 0.5° in magnitude and phase, respectively.

A separate 40-GHz comb generator has also been measured and found to exhibit similar stability characteristics with the same temperature change. When we elevated the 40-GHz generator temperature by 8 K, we saw, by encasing the unit in a
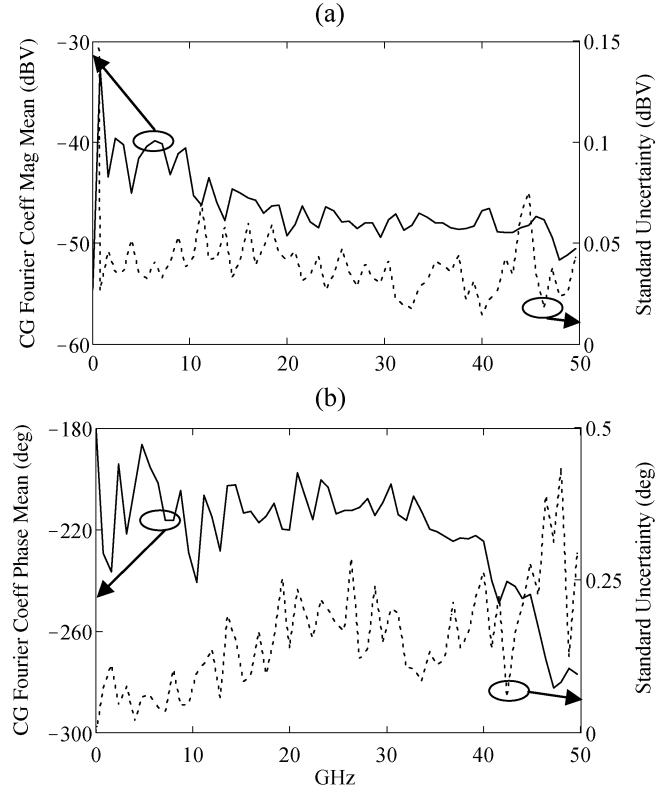


Fig. 9. Comb generator Fourier coefficient mean and standard uncertainty from five identical measurements taken days apart on the two plug-ins. The robust algorithm is used. (a) Magnitude (decibel). (b) Phase.

polystyrene enclosure for a long period, phase changes of up to 1.5° at 40 GHz.

An independent study of comb generator repeatability [15] presented results on two commercial units that settle to thermally stable operating conditions after 20 min. We concur with these findings, but nevertheless ran the comb generator and its driving source for at least 1 h before taking readings. The laboratory temperature was also maintained to within 2 K.

## E. Further Experimental Issues

In addition to our principal findings, we want to comment on two further points that are relevant to this investigation.

First, the selected voltage offset on the oscilloscope vertical scale, as well as the pulse amplitude, must be considered since they affect the linearity of the sampler diodes. We compared traces with various voltage offsets, which we set from the oscilloscope front panel, to a reference trace with no offset. In the frequency-domain comparisons, a negative offset of 50 mV led to changes of up to −0.5 dB in magnitude at 35 GHz and −1° in phase. For a 50-mV positive offset, we found differences of +0.4 dB and +0.3°, respectively. These changes are comparable with those in [11] and the worst differences seen between different plug-ins on different days, 0.1-dB changes of drive-power level or 5-K temperature changes.

Second, we used a plug-in extender head in one set of experiments. Our results showed small anomalies in the measurements due to the use of this plug-in extender. We discovered that laboratory interference is picked up by a common-mode current path established by the extender cable and the bench ground. While

we found that we could eliminate this interference by use of common-mode chokes or current diversion techniques, we felt that the problem can best be avoided by using the plug-ins only in the mainframe housing.

## IV. CHARACTERIZED COMB GENERATOR AND DISCUSSION

Several aspects of the comb generator stability have been considered. With the drive power of our synthesized reference generator and the laboratory temperature having been carefully controlled, we now present the results of the final five experiments with different plug-ins conducted over a period of two days.

We connected the comb generator, with a 10-dB attenuator at its output, to the reference generator. Both generators were switched on for several hours before readings were taken. We then briefly disconnected the comb generator from the plug-in to perform the oscilloscope's internal calibration. The comb generator was then reconnected to the plug-in, which was always housed in the oscilloscope mainframe.

Fig. 9 plots the mean of the five measurements of the comb generator magnitude and phase Fourier coefficients along with their standard uncertainties. In this final measurement, we achieved a standard $1\sigma$ uncertainty better than 0.1 dB in magnitude (apart from the dc point) and $0.5°$ in phase over the entire 50-GHz band.

## V. CONCLUSION

We have extensively investigated the experimental and data-processing conditions necessary to accurately characterize an electrical comb generator's spectral characteristics. We determined that achieving the best repeatability required use of the robust form of the time-base correction algorithm. This reduced the standard uncertainties caused by long-term drift in the oscilloscope and interchange of the plug-ins by up to 0.23 dB and $1.5°$ compared to processing results by use of the simple form of the algorithm.

Finally, using this robust correction and careful control of the input power, input harmonics, and comb generator temperature, we found that the output spectrum of our comb generator can be measured with a standard uncertainty (1 sigma) of 0.1 dB and $0.5°$ over the entire 50-GHz band.

## ACKNOWLEDGMENT

## REFERENCES

[1] *IEEE Standard for the Measurement of Impulse Strength and Impulse Bandwidth*, ANSI/IEEE Standard 376-1975, Jun. 1992, corrected edition.

[2] J. R. Andrews, "Impulse generator spectrum amplitude measurement techniques," *IEEE Trans. Instrum. Meas.*, vol. IM-25, no. 4, pp. 380–384, Dec. 1976.

[3] J. Verspecht, "Calibration of a measurement system for high frequency nonlinear devices," Ph.D. dissertation, Dept. ELEC., Vrije Univ. Brussels, Brussels, Belgium, 1995.

[4] P. S. Blockley, J. B. Scott, D. Gunyan, and A. E. Parker, "Noise considerations when determining phase of large-signal microwave measurements," *IEEE Trans. Microw. Theory Tech.*, vol. 54, no. 8, pp. 3182–3190, Aug. 2006.

[5] D. F. Williams, H. C. Reader, T. S. Clement, P. D. Hale, J. M. Morgan, S. Vandenplas, J. Verspecht, F. Verbeyst, and M. Vanden Bossche, "Comb-generator characterization with calibrated oscilloscopes," presented at the 2nd Nonlinear Meas. Workshop/60th ARFTG Conf., Washington, DC, Dec. 2002.

[6] P. D. Hale, C. M. Wang, D. F. Williams, K. A. Remley, and J. Wepman, "Compensation of random and systematic timing errors in sampling oscilloscopes," *IEEE Trans. Instrum. Meas.*, vol. 55, no. 6, pp. 2146–2154, Dec. 2006.

[7] NIST Time-Base Correction (TBC) Software Aug. 2007. [Online]. Available: http://www.boulder.nist.gov/div815/HSM_Project/Software.htm

[8] P. D. Hale, T. S. Clement, K. J. Coakley, C. M. Wang, D. C. DeGroot, and A. P. Verdoni, "Estimating the magnitude and phase response of a 50 GHz sampling oscilloscope using the 'nose-to-nose' method," in *55th ARFTG Conf. Dig.*, Jun. 2000, pp. 335–342.

[9] T. S. Clement, P. D. Hale, D. F. Williams, C. M. Wang, A. Dienstfrey, and D. A. Keenan, "Calibration of sampling oscilloscopes with high-speed photodiodes," *IEEE Trans. Microw. Theory Tech.*, vol. 54, no. 8, pp. 3173–3181, Aug. 2006.

[10] A. Dienstfrey, P. D. Hale, D. A. Keenan, T. S. Clement, and D. F. Williams, "Minimum-phase calibration of sampling oscilloscopes," *IEEE Trans. Microw. Theory Tech.*, vol. 54, no. 8, pp. 3197–3208, Aug. 2006.

[11] N. G. Paulter and D. R. Larson, "Sources of uncertainty in the nose-to-nose sampler calibration method," *IEEE Trans. Instrum. Meas.*, vol. 52, no. 5, pp. 1618–1626, Oct. 2003.

[12] C. M. Wang, P. D. Hale, and K. J. Coakley, "Least-squares estimation of time-base distortion of sampling oscilloscopes," *IEEE Trans. Instrum. Meas.*, vol. 48, no. 6, pp. 1324–1332, Dec. 1999.

[13] D. F. Williams, T. S. Clement, P. D. Hale, and A. Dienstfrey, "Terminology for high-speed sampling-oscilloscope calibration," in *68th ARFTG Microw. Meas. Conf. Dig.*, Boulder, CO, Nov. 30–Dec. 1 2006, pp. 9–14.

[14] *Guide to Expression of Uncertainty in Measurement*, 1st ed.  Geneva, Switzerland: Int. Org. Standardization, 1993, p. 10.

[15] J. A. Jargon, D. C. DeGroot, and D. F. Vecchia, "Repeatability study of commercial harmonic phase standards measured by a nonlinear vector network analyzer," in *62nd ARFTG Microw. Meas. Conf. Dig.*, Dec. 4–5, 2003, pp. 243–258.

**Howard Charles Reader** received the Ph.D. degree from St. John's College, Cambridge, U.K., in 1985.

From 1986 to 1994, he was a Lecturer, a Senior Lecturer, and an Associate Professor with the University of Natal, Natal, South Africa. In 1994, he became the Chair of High Frequency Electronics, Electrical and Electronic Engineering Department, University of Stellenbosch, Stellenbosch, South Africa. His research interests include electromagnetic compatibility, high-frequency metrology, and microwave dielectric heating. His current research is directed towards the EMI characterization of South Africa's Square Kilometer Array bid.

Dr. Reader is a Chartered Engineer in the U.K. He is a member of the Institution of Engineering and Technology. He serves as South Africa's Union Radio-Scientifique Internationale Commission E (EMI) chair.
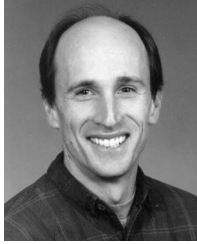
**Dylan F. Williams** (M'80–SM'90–F'02) received the Ph.D. degree in electrical engineering from the University of California at Berkeley, in 1986.

In 1989, he joined the Electromagnetic Fields Division, National Institute of Standards and Technology (NIST), Boulder, CO, where he develops metrology for the characterization of monolithic microwave integrated circuits and electronic interconnects. He has authored or coauthored over 80 technical papers.

Dr. Williams is co-editor-in-chief of the IEEE TRANSACTIONS ON MICROWAVE THEORY AND TECHNIQUES. He was the recipient of the Department of Commerce Bronze and Silver Medals, two Electrical Engineering Laboratory's Outstanding Paper Awards, two Automatic RF Techniques Group (ARFTG) Best Paper Awards, the ARFTG Automated Measurements Technology Award, and the IEEE Morris E. Leeds Award.

**Paul D. Hale** (M'01–SM'01) received the Ph.D. degree in applied physics from the Colorado School of Mines, Golden, CO, in 1989.

Since 1989, he has been with the Optoelectronics Division, National Institute of Standards and Technology (NIST), Boulder, CO, where he conducts research on broadband opto-electronic device and signal metrology. He has been Leader of the High-Speed Measurements Project of the Sources and Detectors Group since 1996. He has authored or coauthored over 50 technical publications. His current technical research focuses on extending both time- and frequency-domain opto-electronic measurements to beyond 110 GHz, implementing a novel covariance-based uncertainty analysis that can be used for both time- and frequency-domain quantities, and disseminating NIST traceability through high-speed electronic and opto-electronic measurement services.

Dr. Hale was an associate editor of optoelectronics/integrated optics for the IEEE JOURNAL OF LIGHTWAVE TECHNOLOGY from June 2001 to March 2007. He was the recipient of the Department of Commerce Bronze, Silver, and Gold Awards, two ARFTG Best Paper Awards, and the NIST Electrical Engineering Laboratory's Outstanding Paper Award.

**Tracy S. Clement** (S'89–M'92–SM'05) received the Ph.D. degree in electrical engineering from Rice University, Houston, TX, in 1993. Her doctoral research involved the development and study of a variety of ultrashort pulse and very short wavelength lasers.

Since 1998, she has been with the Optoelectronics Division, National Institute of Standards and Technology (NIST), Boulder, CO. Her current research interests include the development of measurement systems for high-speed electrooptic components, as well as ultrashort pulse laser measurements. Prior to joining the Optoelectronics Division, she was an Associate Fellow of the Joint Institute for Laboratory Astrophysics (JILA), the Quantum Physics Division, NIST, and was an Assistant Professor Adjoint with the Department of Physics, University of Colorado at Boulder. From 1993 to 1995, she was a Director's Post-Doctoral Fellow with the Los Alamos National Laboratory, Los Alamos, NM.